

---

# ACCELERATED VIDEO ANNOTATION DRIVEN BY DEEP DETECTOR AND TRACKER

---

A PREPRINT

Eric Price<sup>1,2</sup>

Aamir Ahmad<sup>1,2</sup>

<sup>1</sup> Institute for Flight Mechanics and Controls, University of Stuttgart, Germany  
{eric.price,aamir.ahmad}@ifr.uni-stuttgart.de

<sup>2</sup> Max Planck Institute for Intelligent Systems, Tübingen, Germany.

2023-02-19

## ABSTRACT

Annotating object ground truth in videos is vital for several downstream tasks in robot perception and machine learning, such as for evaluating the performance of an object tracker or training an image-based object detector. The accuracy of the annotated instances of the moving objects on every image frame in a video is crucially important. Achieving that through manual annotations is not only very time consuming and labor intensive, but is also prone to high error rate. State-of-the-art annotation methods depend on manually initializing the object bounding boxes only in the first frame and then use classical tracking methods, e.g., adaboost, or kernelized correlation filters, to keep track of those bounding boxes. These can quickly drift, thereby requiring tedious manual supervision. In this paper, we propose a new annotation method which leverages a combination of a learning-based detector (SSD) and a learning-based tracker (RE<sup>3</sup>). Through this, we significantly reduce annotation drifts, and, consequently, the required manual supervision. We validate our approach through annotation experiments using our proposed annotation method and existing baselines on a set of drone video frames. Source code and detailed information on how to run the annotation program can be found at <https://github.com/robot-perception-group/smarter-labelme>

## 1 Introduction

To annotate ground-truth of objects in a video, the annotator must solve two tasks. First, detection of new relevant object instances in each video frame. Second, tracking of already known object instances in subsequent video frames. A graphical user interface (GUI) helps human annotators with these tasks. It can display all relevant information and allow the user to add and modify annotations as quickly as possible. Using visual detection to pre-annotate data - either on the fly or in a preprocessing step - is also common [1, 2]. State-of-the-art open-source programs, like *Smart-labelme* [3], are particularly promising for the purpose of video annotations, since they implements tracking of already annotated objects across frames using classical tracking methods, e.g., adaboost, or kernelized correlation filters. Such trackers often suffer from “drift”. What the tracker considers as a part of the object or not can change in every frame, e.g., a tracker initialized to track a person might drift to eventually track only his/her head or a similar visually easy-to-distinguish part.

In this paper, we present a new annotation method, *Smarter-labelme*, by combining a deep learning-based tracker with a deep learning-based detector that compensates for this drift. While, such techniques have been used for visual tracking methods, to the best of our knowledge they have not been introduced for a freely-available video annotation tool. Furthermore, the visual detector in our method also address the challenge of detecting new and relevant objects to begin with. In our approach, the initial detection is aided by applying SSD-Multibox detector, pre-trained on the MSCOCO dataset on a diverse set of common object classes. The detector is applied in a hierarchical overlapping sliding window technique with global, exclusive, non-maximum suppression to avoid re-detecting already-annotated object instances, truncated objects or multiple detections per object. Instances are assigned a globally unique ID consisting of the detected class name and unique random numeric identifier. For tracking, we use Re<sup>3</sup>, to pre-calculate probable bounding box annotations. SSD-Multibox detector is then used to correct this bounding box for drift if a detection with sufficiently high confidence and Jaccard overlap is found. Annotations are stored in per-video-frame JSON files with consistent instance labels over time. This allows post-processing of annotations, including fine-tuning of the networks that use the annotated data.

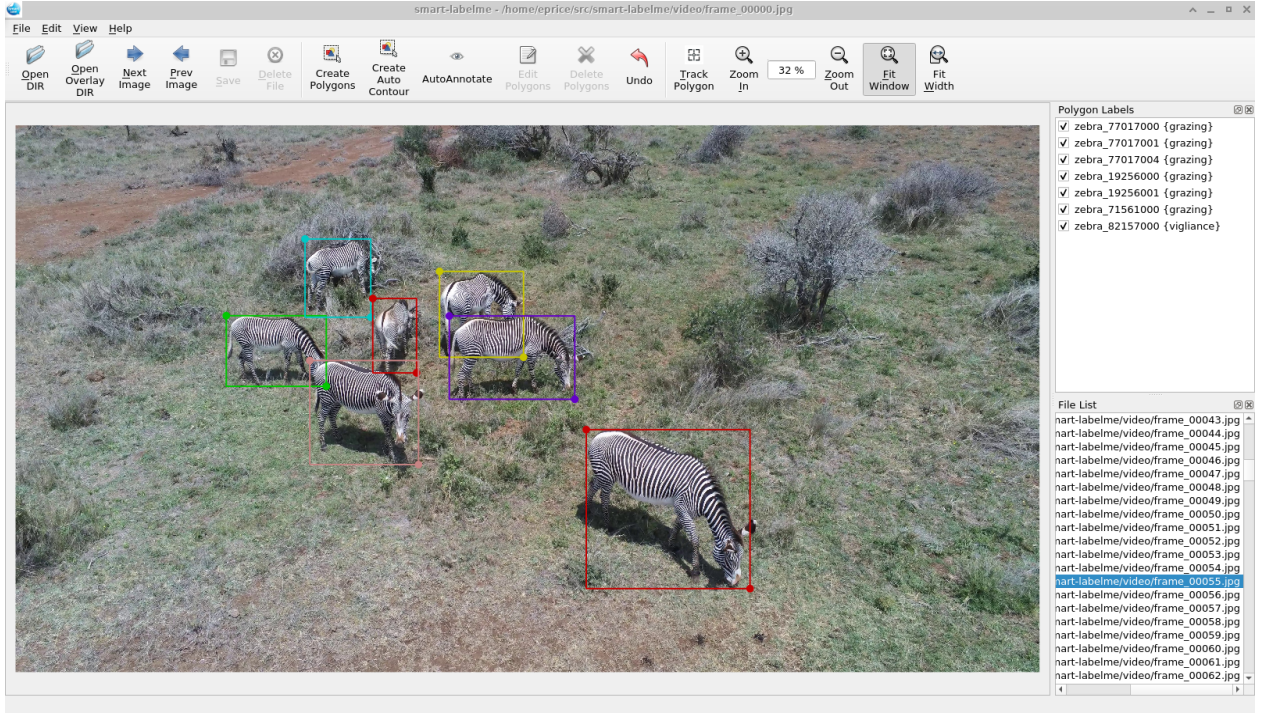


Figure 1: Screenshot of *Smarter-labelme* using SSD-Multibox to auto annotate zebras.

## 2 Related Works

Techniques and tools for video annotation have been extensively studied and applied [1]. Several approaches use cloud-based computation to crowd-source annotation. However, internet bandwidth considerations limit the usability on video. Recent works on video annotation [4] exploit computer vision aided interpolation between human annotated key frames. In this work, we extend *labelme* [5], an open source video annotation tool which has recently been improved [3] to automatically track objects using a traditional computer vision technique provided by OpenCV [2, 6] and is now called *Smart-labelme*. We build on this tool with state-of-the-art methods for both object detection and tracking. Visual object tracking in video has also been extensively studied [7, 8]. Our choice is a light weight network,  $Re^3$  [9], that uses a recurrent siamese approach. Deep convolutional networks have also revolutionized visual object detection [10, 11]. For bounding box detection, we use SSD-Multibox [12], since it has a good tradeoff between speed and accuracy. This network is no longer state-of-the-art mainly due to bad performance on very small objects, but we can circumvent this shortcoming by optimal scaling of detection regions for object tracking, inspired by [13] and within a multi-scale sliding window object detection approach, inspired by [14]. However, instead of parallelizing the detection on specialized hardware, we run the detection neural network sequentially on image regions and only pool the bounding boxes, which allows the algorithm to run efficiently on both GPU and CPU.

## 3 Methodology

### 3.1 Notation

A **Video** is a sequence of  $F$  image frames at frame number  $f$ . We write

$$\mathbf{Video} = (i_f)_{0 \leq f < F}. \quad (1)$$

The **Video** is to be annotated with **Annotations**

$$\mathbf{Annotations} = (\hat{a}_f)_{0 \leq f < F}. \quad (2)$$

Each image frame  $i_f$  is an array of pixels with width  $X$ , height  $Y$  holding a 3 dimensional pixel vector  $\mathbf{p} = [p_R \ p_G \ p_B]^\top$  with pixel brightness values for Red, Green and Blue (RGB)

$$i_f = (\mathbf{p}_{x,y})_{0 \leq x < X, 0 \leq y < Y} \quad (3)$$

where  $[x = 0 \ y = 0]^\top$  is the upper left corner.

Each annotation vector  $\hat{a}_f$  at frame  $f$  consists of  $A_f$  annotations

$$\hat{a}_f = (\mathbf{a}_{a,f})_{0 \leq a < A_f}. \quad (4)$$

Each annotation  $\mathbf{a}_{a,f}$  includes a label  $l_a$  and location vector  $\mathbf{b}_{a,f}$

$$\mathbf{a}_{a,f} = \{l_a, \mathbf{b}_{a,f}\}. \quad (5)$$

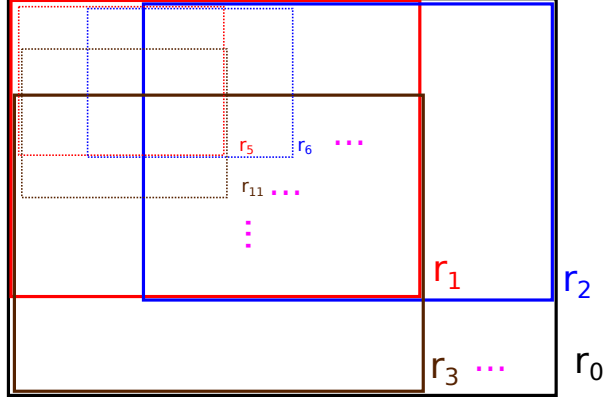


Figure 2: Tiling an image into an array of overlapping tiles at different scales.

While *labelme* [5] supports polygonal annotations for semantic segmentation, both *Smart-labelme* [3] and our solution track instances by their bounding box. Polygonal annotations are scaled in  $x$  and  $y$  direction based on the bounding box size and shape. Therefore, each  $\mathbf{b}$  is a vector with

$$\mathbf{b} = [x_b \ y_b \ X_b \ Y_b]^\top \quad (6)$$

where  $[x_b \ y_b]^\top$  encodes the upper left corner and  $[X_b \ Y_b]^\top$  encodes the width and height of the rectangular bounding box in pixels.

The label  $l$  is a textual representation, which can be used to store information about the annotated object instance, such as its type, identity, etc.

A crop  $C()$  is a sub-image that is a part of a larger image  $i$ . We define  $C()$

$$C(i, \mathbf{b}) = (\hat{e}_{x_c, y_c}) = (\mathbf{p}_{(x_c+x_b), (y_c+y_b)}_{0 \leq x_c < X_b, 0 \leq y_c < Y_b}) \quad (7)$$

as the tensor that maps the submatrix of a frame  $i$  defined by the bounding box coordinates of  $\mathbf{b}$ . While  $C()$  is only defined within the dimensions of  $i$ , we define  $C_0()$  such that pixels outside of the dimensions of  $i$  are simply considered black ( $p_R = p_G = p_B = 0$ ).

Similar, a scale  $S()$  is an image similar to another image  $i$ , which has its resolution changed to  $[X_s \ Y_s]^\top$ . This can be defined by a remapping of pixel coordinates with tensor  $S()$

$$S(i, [X \ Y]^\top, [X_s \ Y_s]^\top) = (\hat{s}_{x_s, y_s}) = (\mathbf{p}_{(\lfloor x_s \frac{X}{X_s} \rfloor), (\lfloor y_s \frac{Y}{Y_s} \rfloor)})_{0 \leq x_s < X_s, 0 \leq y_s < Y_s}, \quad (8)$$

where  $\lfloor \cdot \rfloor$  rounds to the smaller integer. For both tensors, there are matching functions  $c()$ ,  $s()$  and their inverse  $c^{-1}()$ ,  $s^{-1}()$  to map pixel coordinates  $[x \ y]^\top$  or a bounding box  $\mathbf{b}_0 = [x_{b0} \ y_{b0} \ X_{b0} \ Y_{b0}]^\top$  between the image and the crop/scale with

$$[x_c \ y_c]^\top = c([x \ y]^\top, \mathbf{b}) = [(x - x_b) \ (y - y_b)]^\top, \quad (9)$$

$$\mathbf{b}_c = c(\mathbf{b}_0, \mathbf{b}) = [(x_{b0} - x_b) \ (y_{b0} - y_b) \ X_{b0} \ Y_{b0}]^\top, \quad (10)$$

$$[x_s \ y_s]^\top = s([x \ y]^\top, [X \ Y]^\top, [X_s \ Y_s]^\top) = \left[ \left( x \frac{X_s}{X} \right) \ \left( y \frac{Y_s}{Y} \right) \right]^\top, \quad (11)$$

$$\mathbf{b}_s = s(\mathbf{b}_0, [X \ Y]^\top, [X_s \ Y_s]^\top) = \left[ \left( x_{b0} \frac{X_s}{X} \right) \ \left( y_{b0} \frac{Y_s}{Y} \right) \ \left( X_{b0} \frac{X_s}{X} \right) \ \left( Y_{b0} \frac{Y_s}{Y} \right) \right]^\top. \quad (12)$$

Note: In practice, for  $S()$  we use interpolating methods implemented in both OpenCV and PyTorch to avoid aliasing effects.

### 3.2 Multi Scale Tiling Approach

A common approach in computer vision is to divide the image  $i$  systematically into overlapping tiles of different size. This is used among others by [12, 14] and also the majority of Deep Convolutional Neural Networks (CNN).

A visual operation, for example feature or object detection, can then be executed in parallel on all these tiles, across the image at both large and small scale. The approach is also called an ‘‘Optical Pyramid’’ and can be considered a manifestation of the ‘‘divide and conquer’’ paradigm often found in computer science. If a tile  $r$  has size  $[X_r \ Y_r]^\top$ , then  $r_0$  would typically represent the whole image with

$$r_0 = S(i, [X \ Y]^\top, [X_r \ Y_r]^\top). \quad (13)$$

All other tiles are based on a cropped tile area  $\mathbf{b}_n = [x_{b_n} \ y_{b_n} \ X_{b_n} \ Y_{b_n}]^\top$

$$\mathbf{r}_n = \mathcal{S} \left( \mathcal{C}(\mathbf{i}, \mathbf{b}_n), [X_{b_n} \ Y_{b_n}]^\top, [X_r \ Y_r]^\top \right) \quad (14)$$

The tiling, shown in Fig. 2 is typically done with a recursive algorithm that calculates all  $\mathbf{b}_n$  for different sizes to cover the whole image space. This can be either overlapping or non-overlapping depending on the use case. Typically every layer of tiles has approximately 4 times the tiles as the previous at half the tile dimensions, while the number of layers depends on the resolution of the original image and the minimum tile size. The latter is often identical to  $[X_r \ Y_r]^\top$  and yields an array of  $R$  tile boxes  $\mathbf{T}$  with

$$\mathbf{T} = (\mathbf{b}_r)_{0 \leq r < R} = \mathbf{Tile} \left( [X \ Y]^\top, [X_r \ Y_r]^\top \right). \quad (15)$$

### 3.3 Manual Annotation

*Labelme* [5] is optimized to streamline the process for human annotators. One video frame  $i_f$  is always displayed prominently on the screen. The user can navigate between frames with the arrow keys on the keyboard and in the spacial dimension with keyboard + scroll wheel, which allows very fast navigation. Ctrl + scroll wheel can zoom in or out to magnify areas in high resolution images, while the Alt key or no key are used to pan horizontally or vertically. Navigating to a specific  $f$  can be done fast by mouse-click on a timeline which highlights all frames already annotated. The user can add annotations by entering the appropriate mode (Ctrl+R) and then clicking diagonally opposite corners of a rectangle. A prompt box will appear in which the user can select or type a label for the new annotation. The previous annotation is pre-selected which is very fast if many identical labels are given. However, modification of the label is necessary if every instance is supposed to receive distinct identifiers. For the latter case, an experienced and well rested annotator can achieve a speed of under 5 seconds per annotation. For identical labels, a speed of under 4 seconds is possible. These values are approximate, evaluated in self-test and can increase drastically depending on the visual difficulty of the individual annotation task.

### 3.4 Assisted Tracking

*Smart-labelme* [3] adds the ability to track objects between subsequent frames using a method for parametric image alignment [2], which is implemented in the OpenCV library [6]. Using this to track objects works, if these are visually distinctive and do not change appearance drastically. The method is not well suited to track organic structures that undergo morphological changes such as a bird flapping its wings or a horse moving its legs while walking. The process involves selecting one or more existing annotations and then clicking “track-polygon”. When the user then navigates to a different video frame which does not yet have an annotation with the same labels, the tracking algorithm is applied to find the corresponding bounding box in the new frame and creating new object annotations. Even if the tracking is imperfect, the human annotator only needs to adjust bounding box corners for existing annotations, with no need to type. The algorithm runs sequentially on CPU and is comparably slow. The annotations in the first video frame  $\hat{\mathbf{a}}_0$  need to be made manually as described in Sec. 3.3.

### 3.5 Assisted Tracking with $\text{Re}^3$

$\text{Re}^3$  [9] is a recurrent siamese network, utilizing Long-term-Short-term memory (LSTM) nodes to remember the appearance of tracked object instances, while simultaneously observing two cropped images.  $\mathcal{C}(i_f, \tilde{\mathbf{b}}_{a,f}), \mathcal{C}(i_{f+1}, \tilde{\mathbf{b}}_{a,f})$ . Since  $\text{Re}^3$  has internal memory, for each annotation  $\mathbf{a}_{a,f}$  we also need to store internal memory  $\mathbf{R}_{a,f}$ , which will be updated by the tracker in every tracking transition. We can represent  $\text{Re}^3$  as a function, based on a crop region  $\tilde{\mathbf{b}}_{a,f}$  as

$$\left\{ \hat{\mathbf{b}}_{a,f+1}, \mathbf{R}_{a,f+1} \right\} = \text{Re}^3 \left( \mathcal{C}_0(i_f, \tilde{\mathbf{b}}_{a,f}), \mathcal{C}_0(i_{f+1}, \tilde{\mathbf{b}}_{a,f}), \mathbf{R}_{a,f} \right). \quad (16)$$

$\text{Re}^3$  provides the new coordinates  $\hat{\mathbf{b}}_{a,f+1}$  for the tracked objects in the new cropped region corresponding to a object that occupies the exact center in the old cropped region. For any annotation  $\mathbf{a}_{a,f} = \{l_a, \mathbf{b}_{a,f}\}$  and  $\mathbf{b}_{a,f} = [x_b \ y_b \ X_b \ Y_b]^\top$  the crop region is always twice as large as the to be tracked object instance, with

$$\tilde{\mathbf{b}}_{a,f} = [x_{\tilde{b}} \ y_{\tilde{b}} \ X_{\tilde{b}} \ Y_{\tilde{b}}] = \left[ \left( x_b - \left\lfloor \frac{X_b}{2} \right\rfloor \right) \ \left( y_b - \left\lfloor \frac{Y_b}{2} \right\rfloor \right) \ 2X_b \ 2Y_b \right]^\top. \quad (17)$$

Which leads to annotation  $\mathbf{a}_{a,f+1}$  based on  $\hat{\mathbf{b}}_{a,f+1} = [x_{\hat{b}} \ y_{\hat{b}} \ X_{\hat{b}} \ Y_{\hat{b}}]^\top$  and  $\tilde{\mathbf{b}}$

$$\mathbf{a}_{a,f+1} = \left\{ \left[ (x_{\hat{b}} + x_{\tilde{b}}) \ (y_{\hat{b}} + y_{\tilde{b}}) \ X_{\hat{b}} \ Y_{\hat{b}} \right]^\top, l_a \right\}. \quad (18)$$

If  $\mathbf{R}_{a,f}$  is not known, we first initialize the tracker with

$$\{\dots, \mathbf{R}_{a,f}\} = \text{Re}^3 \left( \mathcal{C}_0(i_f, \tilde{\mathbf{b}}_{a,f}), \mathcal{C}_0(i_f, \tilde{\mathbf{b}}_{a,f}), \mathbf{0} \right). \quad (19)$$

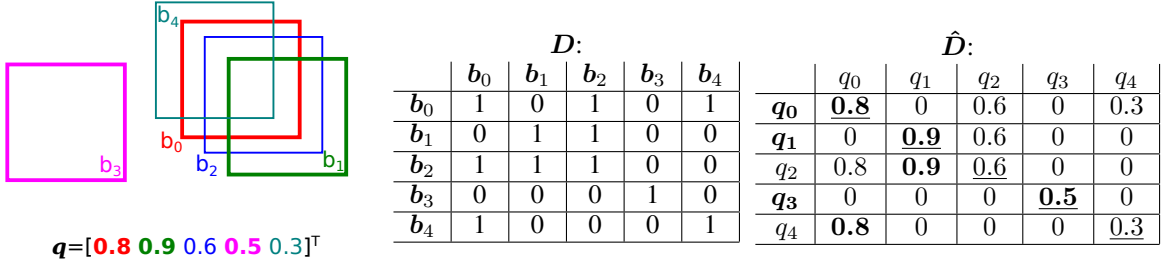


**Figure 3:** Matrices  $D$  and  $\hat{D}$  for example detections  $\mathbf{b}$  with confidence scores  $\mathbf{q} = [0.8 \ 0.9 \ 0.6 \ 0.5 \ 0.3]^T$ . NMS is performed by selecting only those  $b_n$  for which  $q_n$  (underlined) equals the row-maximum (**bold**).

This allows tracking equivalent to *Smart-labelme* but using a modern, fast, recurrent deep convolutional method. Re<sup>3</sup> suffers from drift, but drift only manifests itself after some time, at which the user might have to adjust the bounding box manually to correct for the error.

### 3.6 Assisted Detection with SSD-Multibox

SSD-Multibox is a Deep Convolutional Neural Network (CNN) for object detection. It operates with a fixed input size  $[X_r \ Y_r]^T$  of 300px  $\times$  300px. This input image is divided using **Tile** into  $T_{\text{SSD}} = 8732$  overlapping receptive fields, called prior boxes. For each such box the network outputs  $\mathbf{o}_n$  with  $\mathbf{b}_n = [x_{b_n} \ y_{b_n} \ X_{b_n} \ Y_{b_n}]^T$  for a potential object instance candidate, as well as  $K$  confidence scores  $\mathbf{k}_n$  used for classification into  $K$  object classes, so

$$(\mathbf{o}_n)_{0 \leq n < T_{\text{SSD}}} = \text{SSD}(\mathbf{i}) \quad (20)$$

with

$$\mathbf{o}_n = \{\mathbf{b}_n, \mathbf{k}_n\}. \quad (21)$$

Typically non-maximum suppression (NMS) is applied to only report the most confident of any overlapping array of detections for each class. However, we defer this step. When analyzing high resolution video, it is not practical to downscale each frame to the network resolution. Instead we apply **Tile** to divide each image frame  $\mathbf{i}_f$  into  $D$  overlapping tiles  $\mathbf{b}_d = [x_{b_d} \ y_{b_d} \ X_{b_d} \ Y_{b_d}]^T$ , then run SSD on each so

$$\mathbf{i}_{f,d} = \mathcal{S} \left( \mathcal{C}(\mathbf{i}_f, \mathbf{b}_d), [X_{b_d} \ Y_{b_d}]^T, [X_r \ Y_r]^T \right) \forall \mathbf{b}_d \in \text{Tile} \left( [X \ Y]^T, [X_r \ Y_r]^T \right). \quad (22)$$

In each array of detections  $\text{SSD}(\mathbf{i}_{f,d})$ , we discard any detections that are close to the edges of  $\mathbf{i}_{f,d}$ , since these detections are likely truncated. Since tiles are overlapping at different scales, there always exists another tile that covers the whole object instance. We apply  $c^{-1}()$  and  $s^{-1}()$  to transform the remaining bounding boxes into the coordinate frame of  $\mathbf{i}_f$  to compute  $\hat{\mathbf{o}}_f$  with

$$\hat{\mathbf{o}}_f = \bigcup_{0 \leq d < D} c^{-1} \left( s^{-1}(\text{remove.truncated}(\text{SSD}(\mathbf{i}_{f,d}))) \right). \quad (23)$$

**3.6.1 Non Maximum Suppression** Storing  $\hat{\mathbf{o}}_f$  in a PyTorch tensor, we loop through each of  $K$  object classes. For each class, we sort  $\hat{\mathbf{o}}_f$  by confidence score and truncate the  $L = 5000$  highest confidence detections. This puts an upper bound on the computational effort. We then have  $L$  bounding boxes  $\mathbf{b} = (\mathbf{b}_l)_{0 \leq l < L}$  and  $L$  confidence scores  $\mathbf{q} = (q_l)_{0 \leq l < L}$ . We calculate  $\mathbf{J} = (j)_{m,n}$  which is an  $L \times L$  matrix of the intersection over union (IOU) of these bounding boxes. We derive  $D$  as a boolean  $L \times L$  matrix with

$$D = \left( d_{m,n} = \begin{cases} 1 & \iff j_{m,n} > 0.5 \\ 0 & \iff j_{m,n} \leq 0.5 \end{cases} \right)_{0 \leq m < L, 0 \leq n < L}, \quad (24)$$

from which we calculate  $\hat{D}$  by column wise multiplication with  $\mathbf{q}$  with

$$\hat{D} = \left( \hat{d}_{m,n} = q_n d_{m,n} \right)_{0 \leq m < L, 0 \leq n < L}. \quad (25)$$

As illustrated in Fig. 3. Maxima are those  $\{\mathbf{b}_l \ q_l\}$  for which the maximum of the  $l$ th row-vector of  $\hat{D}$  is identical to  $q_l$  itself, i.e. the row-maximum is on the diagonal of  $\hat{D}$ .

Crucially, this entire algorithm can be expressed in PyTorch tensor operations and computed in a parallel on GPU with constant computational runtime. This is substantially faster than typical iterative looping algorithms for NMS, especially when implemented in Python.

For automatic annotation, we extend NMS by also excluding any detections that have an IOU  $\geq 0.5$  with existing  $\mathbf{a}_{a,f} \in \hat{\mathbf{a}}_f$ . We add any remaining detections, computing a new  $\mathbf{l}_a$  using the SSD class  $k$  and a unique number computed from the system time and a counter.

### 3.7 Drift-compensation with SSD-Multibox and Re<sup>3</sup>

For each Re<sup>3</sup> invocation, we run SSD on each  $\tilde{b}_{a,f}$ . If a detection is found (21) that has an IOU with  $\hat{b}_{a,f+1}$  as computed by Re<sup>3</sup> (16) of 0.8 or higher, regardless of class, then we assume SSD found the object instance. We then correct  $b_{a,f+1}$  using a weighed average of both SSD and Re<sup>3</sup> prediction and copy the label to compute  $\hat{a}_{f+1}$ .

## 4 Experiments

### 4.1 Method Variants

**4.1.1 Baseline** The baseline variant does not aid the annotator with any computer vision technique. Annotations  $\hat{a}_0$  need to be annotated by hand. In the original *labelme* [5], no tracking variant exists, and labels need to be manually copied to the next frame. However, this is needless overhead and would not be suitable to evaluate the impact of machine accelerated tracking. Therefore, we implemented a pseudo-tracker that copies the current annotations to the next frame with  $\hat{a}_{f+1} = \hat{a}_f$  when engaged. This keeps the work flow identical to the variants with a real tracker, however, the user needs to then manually correct each bounding box in all subsequent frames, unless the object instance has remained stationary.

**4.1.2 OpenCV** The OpenCV variant is *Smart-labelme* [3] as described in Sec. 3.4 using parametric image alignment to track object instances.

**4.1.3 Ours** Our variant, *Smarter-labelme*, uses Re<sup>3</sup> with SSD-Multibox drift compensation as described in Sec. 3.7 to track, and the Auto-Annotation function described in Sec. 3.6 is available to the annotator to help annotate  $\hat{a}_0$ .

### 4.2 Experiment Setup

We setup a computer with the method variants and allowed multiple annotators to perform a video annotation task with each. For a fair comparison, all experiments were conducted on the same computer equipped with a modern AMD Ryzen CPU and NVIDIA GPU and a 4K monitor. The annotated video, shown in Fig. 4 was a short 4K aerial clip of 8 horses walking on a snowy plane, shot using one of our aerial robots. Each annotator was provided with an introduction and demonstration of the labeling tool, followed by a 5 minute practice period to familiarize themselves with the tool and the annotation process. Then all annotations were reset and the program restarted. Each annotator was given 10 minutes to annotate the video for each of the 3 variants (i.e., 30 min in total). After ten minutes, the variant was switched and all annotations reset. The order in which variants were evaluated was randomized to minimize bias introduced by exhaustion or increased proficiency. The annotators were instructed to annotate with consistent accuracy throughout the experiments. The number of successfully annotated object instances were counted for each method variant and annotator.

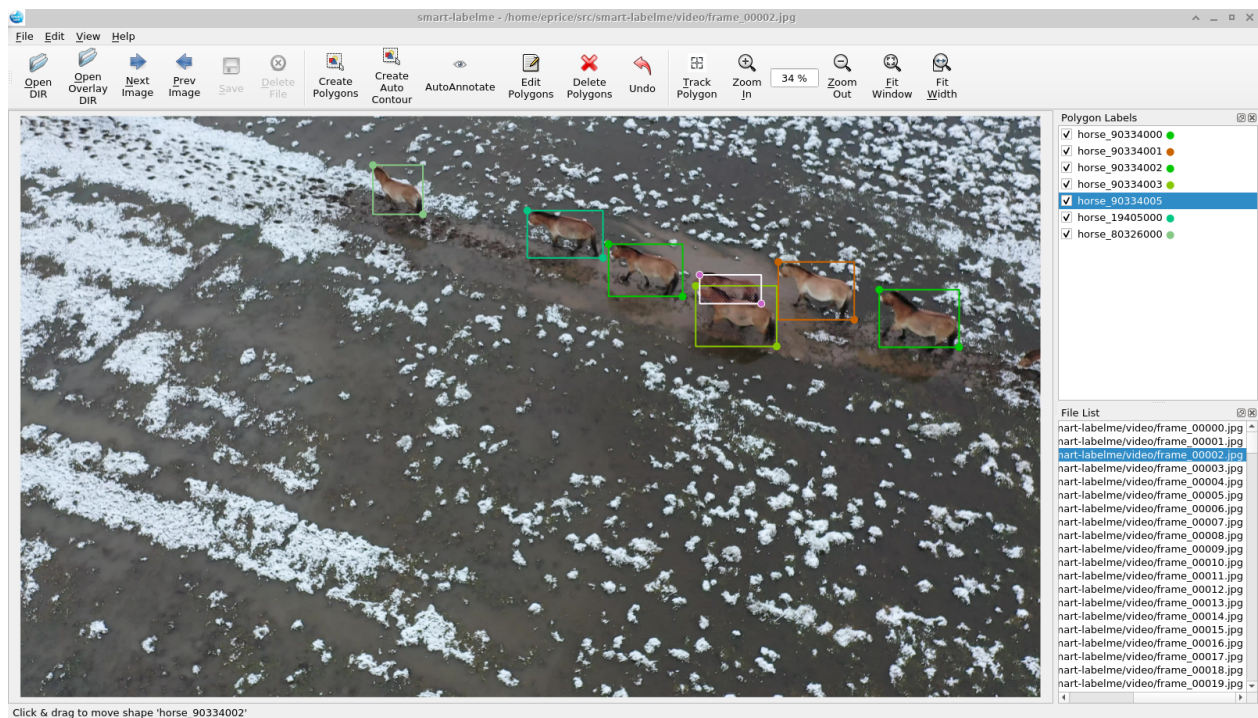


Figure 4: Screenshot of the experiment. Annotation of a video with walking horses.

**Table 1:** Results of the annotation experiments.

Annotator	Seq.	Exp.	Frames	Annotations	Speedup
1	1	Baseline	6	41	1.0
	2	<b>Ours</b>	<b>8</b>	<b>62</b>	<b>1.51</b>
	3	OpenCV	7	56	1.37
2	1	OpenCV	6	48	0.86
	2	<b>Ours</b>	<b>8</b>	<b>69</b>	<b>1.23</b>
	3	Baseline	7	56	1.0
3	1	<b>Baseline</b>	<b>6</b>	<b>44</b>	<b>1.0</b>
	2	OpenCV	5	40	0.91
	3	Ours	5	38	0.86
4	1	<b>Ours</b>	<b>16</b>	<b>128</b>	<b>1.08</b>
	2	Baseline	15	118	1.0
	3	OpenCV	14	105	0.89
5	1	OpenCV	9	72	0.81
	2	<b>Baseline</b>	<b>12</b>	<b>89</b>	<b>1.0</b>
	3	Ours	11	86	0.97
Mean		OpenCV	8.2	64.2	0.97
		Baseline	9.2	69.6	1.0
		<b>Ours</b>	<b>9.6</b>	<b>72.6</b>	<b>1.13</b>

## 5 Results and Discussion

We conducted experiments as described in Sec. 4.2 with 5 different human annotators. The results are shown in Table 1. On that video, the annotators achieved on average 13% faster annotation speeds with our method than the baseline. *Smart-labelme* [3] using OpenCV was on average 3% slower than the baseline. As seen in Fig. 5, there were noticeable differences between the annotators. Annotator 3 reported, that they spent a lot of time re-labeling and correcting auto annotations made with SSD-Multibox in the first frame, which had a comparably large impact due to their slow annotation speed. All annotators did manual corrections to the trackers labels in every frame as needed, but consistently reported that this process took longer if the tracking error was larger. This explains why the baseline method, which simply copies the previous frames labels to the next outperformed OpenCV, which had a tendency to occasionally make large tracking errors. Another contributing factor was the long processing time of OpenCV which added several seconds to every annotated frame. The deep methods tracked significantly faster since they used GPU and were more accurate, while the baseline did not spend any time processing between frames.

The experiments show that using our proposed approach, we can speed up the annotation process, while keeping the processing overhead low. Secondly, humans are faster with a trivial method (copying bounding boxes and manually adjusting them) than correcting a bad automatic label. During tests we also found cases where, in a complex scene, a large number of objects were tracked correctly, while some objects due to their visual appearance, upset the tracker and resulted in consistent bad labels. The annotation tool should, therefore, allow the annotator to disable the accelerated tracker for individual objects if they notice such a malfunction, and revert to the trivial method of copying bounding boxes between frames. We have therefore added this functionality to our open source implementation.

The benefit of our approach depends greatly on the required annotation quality. In our experiment, the annotators aspired to make pixel exact annotations which required careful monitoring and corrections to every bounding box in every frame. If rough annotations are sufficient, both the validation process and the correction - if needed - can be significantly faster. The performance of detector and tracker might often be sufficient for the task. In this case, the processing time of the tracker becomes a major bottleneck for annotation and additional effort is required to optimize the software for speed. On the other hand, if very high quality annotations are needed, the overall speed can increase if the quality of machine accelerated annotations is improved. This can be done by fine-tuning the detector on already annotated data.

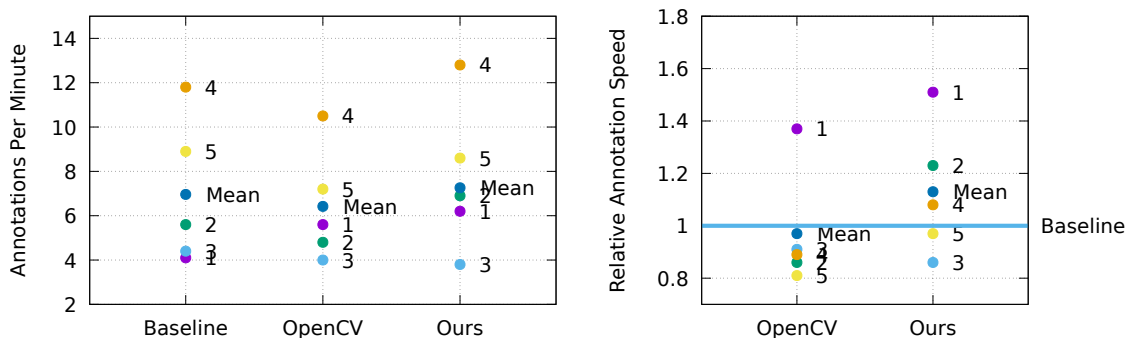


**Figure 5:** Visualized experiment results. The absolute and relative annotation speed of the respective annotators are displayed, compared to baseline.

## 6 Conclusion and Outlook

We presented an accelerated video annotation method for instance labeling in videos. Our method combines deep networks for detection and tracking to reduce drift in annotation over frames, thereby substantially increasing annotation speed. We validated this through experiments where we compared our approach with baseline methods, and discussed how to maximize utility depending on the required accuracy in annotations. We provided open-source code of our method for the benefit of the community. Future work may involve online training of the detector on the objects being tracked in real time, using the already labeled annotations as training data.

## References

- [1] E. Gaur, V. Saxena, and S. K. Singh, "Video annotation tools: A review," in *2018 International Conference on Advances in Computing, Communication Control and Networking (ICACCCN)*, Oct 2018, pp. 911–914. 1, 2
- [2] G. D. Evangelidis and E. Z. Psarakis, "Parametric image alignment using enhanced correlation coefficient maximization," *IEEE Transactions on Pattern Analysis and Machine Intelligence*, vol. 30, no. 10, pp. 1858–1865, Oct 2008. 1, 2, 3.4
- [3] B. Ajani, "Smart-labelme: Video / Image Annotation (Polygon, Semantic mask, Classification) with Python," <https://github.com/bhavyaajani/smart-labelme>, 2020. 1, 2, 3.1, 3.4, 4.1.2, 5
- [4] A. Kuznetsova, A. Talati, Y. Luo, K. Simmons, and V. Ferrari, "Efficient video annotation with visual interpolation and frame selection guidance," in *Proceedings of the IEEE/CVF Winter Conference on Applications of Computer Vision (WACV)*, January 2021, pp. 3070–3079. 2
- [5] K. Wada, "labelme: Image Polygonal Annotation with Python," <https://github.com/wkentaro/labelme>, 2016. 2, 3.1, 3.3, 4.1.1
- [6] I. Culjak, D. Abram, T. Pribanic, H. Dzapo, and M. Cifrek, "A brief introduction to opencv," in *2012 Proceedings of the 35th International Convention MIPRO*, May 2012, pp. 1725–1730. 2, 3.4
- [7] M. Fiaz, A. Mahmood, S. Javed, and S. K. Jung, "Handcrafted and deep trackers: Recent visual object tracking approaches and trends," *ACM Comput. Surv.*, vol. 52, no. 2, apr 2019. [Online]. Available: <https://doi.org/10.1145/3309665> 2
- [8] S. Javed, M. Danelljan, F. S. Khan, M. H. Khan, M. Felsberg, and J. Matas, "Visual object tracking with discriminative filters and siamese networks: A survey and outlook," *IEEE Transactions on Pattern Analysis and Machine Intelligence*, pp. 1–20, 2022. 2
- [9] D. Gordon, A. Farhadi, and D. Fox, "Re<sup>3</sup>: Real-time recurrent regression networks for visual tracking of generic objects," *IEEE Robotics and Automation Letters*, vol. 3, no. 2, pp. 788–795, April 2018. 2, 3.5
- [10] Z. Zou, K. Chen, Z. Shi, Y. Guo, and J. Ye, "Object detection in 20 years: A survey," *Proceedings of the IEEE*, pp. 1–20, 2023. 2
- [11] X. Wu, D. Sahoo, and S. C. Hoi, "Recent advances in deep learning for object detection," *Neurocomputing*, vol. 396, pp. 39–64, 2020. [Online]. Available: <https://www.sciencedirect.com/science/article/pii/S0925231220301430> 2
- [12] W. Liu, D. Anguelov, D. Erhan, C. Szegedy, S. Reed, C.-Y. Fu, and A. C. Berg, "Ssd: Single shot multibox detector," in *Computer Vision – ECCV 2016*, B. Leibe, J. Matas, N. Sebe, and M. Welling, Eds. Cham: Springer International Publishing, 2016, pp. 21–37. 2, 3.2
- [13] E. Price, G. Lawless, R. Ludwig, I. Martinovic, H. H. Bühlhoff, M. J. Black, and A. Ahmad, "Deep neural network-based cooperative visual tracking through multiple micro aerial vehicles," *IEEE Robotics and Automation Letters*, vol. 3, no. 4, pp. 3193–3200, Oct 2018. 2
- [14] H. Nakahara, H. Yonekawa, and S. Sato, "An object detector based on multiscale sliding window search using a fully pipelined binarized cnn on an fpga," in *2017 International Conference on Field Programmable Technology (ICFPT)*, Dec 2017, pp. 168–175. 2, 3.2